Hindawi
International Journal of Antennas and Propagation
Volume 2020, Article ID 1212894, 9 pages
https://doi.org/10.1155/2020/1212894

Research Article

Bandwidth Enhancement on Half-Mode Substrate Integrated Waveguide Antenna Using Cavity-Backed Triangular Slot

Dian Widi Astuti, Muhamad Asvial, Fitri Yuli Zulkifli, and Eko Tjipto Rahardjo

Department of Electrical Engineering, Faculty of Engineering, Universitas Indonesia, Depok 16424, Indonesia

Correspondence should be addressed to Dian Widi Astuti; dian.widi@ui.ac.id and Eko Tjipto Rahardjo; eko@eng.ui.ac.id

Received 29 June 2020; Revised 7 October 2020; Accepted 15 November 2020; Published 3 December 2020

Academic Editor: Hervé Aubert

This paper proposes bandwidth enhancement of a cavity-backed slot antenna using a triangular slot on a half-mode substrate integrated waveguide structure antenna. The bandwidth enhancement was achieved by combining the fixed TE_{101} and the downward shifting TE_{102} modes, resulting in hybrid modes. The design evolution of the slot antenna from a half nonresonating rectangular slot to a triangular slot antenna increased the fractional bandwidth. The simulation result showed that fractional bandwidth increased from 6.27% to 9.1%. It was confirmed by measurement that the fractional bandwidth of 9.87% was achieved which reflects a 350 MHz bandwidth with center frequency at 3.84 GHz. The measured gain at center frequency was 4.2 dBi. It is shown that the radiation characteristics obtained from both measurement and simulation results are in very good agreement.

1. Introduction

Cavity-backed slot (CBS) antennas using the substrate integrated waveguide (SIW) technology provide easy integration in the planar form and enable low-cost fabrication for various applications. To meet the requirements of various applications, researchers have proposed miniaturization, bandwidth enhancement, circular polarization, gain improvement, dual band, and self-diplexing. The miniaturization of the SIW-CBS antenna was proposed in [1–4]. The miniaturization of the SIW-CBS antenna can vertically cut the magnetic field of the full-mode SIW (FMSIW) into two parts of the half-mode substrate integrated waveguide (HMSIW) structure, as shown in [1–4]. By using the HMSIW structure, 50% miniaturization of the antenna was obtained; however, all the fractional bandwidths in [1–4] were below 7%.

Bandwidth enhancements for the SIW-CBS antenna have been proposed in [5–8]. Yun et al. [5] proposed substrate removal under the slot radiator, which successfully enhanced the impedance bandwidth although the bandwidth increased only up to 2.16% of the fractional bandwidth. Researchers have also implemented a hybrid mode or a multiresonance mode to enhance the impedance bandwidth, as shown in [6–8]. A shorting via above the slot creates double resonance, which was implemented to enhance the bandwidth [6]. A 3.35% increase in the fractional bandwidth was achieved using this technique; however, tuning the shorting via location was not an easy task. Luo et al. [7] and Mukherjee et al. [8] presented hybrid resonance using the half cavity of two adjacent resonances between TE_{101} and TE_{102} while TE_{101} was kept as the first mode. However, the fractional bandwidths are still narrow.

In this paper, bandwidth enhancement is proposed using a triangular slot on the HMSIW structure. The triangular slot was etched on the ground layer. The position, length, and width of the triangular slot will be varied to generate the first mode TE_{101} and the second mode TE_{102} closer to each other. Their appropriate combination will result in impedance matching for a hybrid resonance by keeping the first mode TE_{101} fixed and the second mode TE_{102} shifting downward frequency. This provides a significant advantage because the mixing of HMSIW structure together with the triangular slot could effectively enhance the bandwidth to reduce antenna dimensions. Furthermore, the proposed antenna could be used for the fifth-generation telecommunications where its

application needs broad bandwidth characteristic and compact design antenna.

2. Antenna Design

Bandwidth enhancement for a cavity backed by a triangular slot antenna in the HMSIW structure is proposed using a geometric structure, as shown in Figure 1. The triangular slot was etched on the ground layer that acted as a nonresonating slot. The top layer acted as a metallic reflector. The triangular slot excited the first mode TE_{101} at 3.8 GHz and the second mode TE_{102} at 3.98 GHz. Their impedance matched the frequency range as a hybrid resonance.

The geometry evolution to achieve the proposed antenna geometry shown in Figure 1 is depicted in Figures 2(a)–2(c). In the first step, the FMSIW cavity structure with rectangular slot on the ground plane was used, as shown in Figure 2(a). The resonant frequency for the TE_{mnp} mode was calculated using the following equation [9]:

$$f_{mnp} = \frac{c}{2\sqrt{\mu_r \varepsilon_r}} \sqrt{\left(\frac{m}{L_{\text{eff}}}\right)^2 + \left(\frac{n}{h}\right)^2 + \left(\frac{p}{W_{\text{eff}}}\right)^2}, \quad (1)$$

where for the first mode $TE_{101,}$ $m = 1$, $n = 0$, and $p = 1$; c is the velocity of light in free space; h is the substrate thickness; and μ_r and e_r are the relative permeability and relative permittivity of the substrate, respectively. In fact, only the TE_{m0p} modes can resonate in the rectangular SIW and TE_{m0} can be propagated in the SIW waveguide because the transverse magnetic (TM) modes are not supported in the SIW technology owing to the noncontinuous walls [10–12]. The effective length (L_{eff}) and effective width (W_{eff}) of the rectangular cavity are determined as follows [13]:

$$L_{\text{eff}} = L_c - 1.08\frac{D^2}{S} + 0.1\frac{D^2}{L_c},$$
$$W_{\text{eff}} = W_c - 1.08\frac{D^2}{S} + 0.1\frac{D^2}{W_c}, \quad (2)$$

where L_c and W_c are the length and width, respectively, of a rectangular cavity; D is the diameter of the embedded metallic cylinders; S is the distance between the two adjacent center points of the embedded metallic cylinders, and λ_0 is the free space wavelength. The conditions $S/D \leq 2$ and $\lambda_0/D \geq 10$ should be considered to minimize the leakage energy.

The antenna design uses Rogers RT/Duroid 5880 with dielectric relative permittivity $\varepsilon_r = 2.2$, loss tangent $\delta = 0.0009$, and substrate thickness $h = 1.575$ mm. The single-resonant FMSIW structure has one drawback: it has a narrow bandwidth.

The second step of antenna evolution involved miniaturizing and bandwidth enhancement of the SIW-CBS antenna. The miniaturization was achieved by cutting the magnetic wall vertically and making it an HMSIW-CBS antenna, as shown in Figure 2(b). Bandwidth enhancement was achieved using hybrid modes between TE_{101} and TE_{102}. The hybrid modes were achieved by dividing the HMSIW patch into a quarter patch of TE_{101} and TE_{102}. These two modes could be excited by varying the slot length and slot position of the nonresonating slot by a length more than a quarter wavelength. Finally, the bandwidth of the HMSIW-CBS antenna could be enhanced by flaring the rectangular nonresonating slot into a triangular slot, as shown in Figure 2(c).

3. Results and Discussion

3.1. Simulation Study. As depicted in Figure 2, the radiation characteristics of each step evolution are displayed, and simulation study using Ansys HFSS software is considered. Figure 3 shows comparison results of the reflection coefficient for the antenna evolution shown in Figure 2. The fractional bandwidth of FMSIW-CBS is only 1.81% (70 MHz) for 3.86 GHz of center frequency. Furthermore, the fractional bandwidth of HMSIW increases to 6.27% (240 MHz). This HMSIW structure prevents the shifting of the resonant frequency to a lower frequency because the electric field radiates across the dielectric aperture by the first mode TE_{101}. The modification of nonresonating slot into a triangular slot will cause more impedance bandwidth improvement up to 350 MHz, which has 9.1% for fractional bandwidth. It means that the proposed antenna fractional bandwidth increases five times higher than the FMSIW-CBS antenna.

The bandwidth enhancement for a cavity backed by a triangular slot antenna in the HMSIW structure can be explained from the real impedance simulation result, as displayed in Figure 4. It is shown that the first mode TE_{101} and the second mode TE_{102} are close to each other. The hybrid resonances between TE_{101} and TE_{102} will enhance the impedance bandwidth. Hybrid resonance occurs without changing the first resonant mode TE_{101}. The fractional bandwidth was improved to 9.1%. In the real impedance plot, it is shown that the operating band has a wideband as compared with other operating bands.

In addition, the simulated H-field vector distribution corresponds to a combination between the first mode TE_{101} and the second mode TE_{102}, as shown in Figure 5. The simulated H-field vector distributions are illustrated with the same scale of 0–100 A/m. The H-field vector distribution is separated by the triangular slot into a lower quarter cavity part and an upper quarter cavity part. Figure 5(a) shows the simulated H-field vector distribution at 3.8 GHz; the field distributions in both parts are out of phase. The dominant field distribution of the H-field vector is located in the lower cavity. Figure 5(b) shows the simulated H-field vector distribution at 3.98 GHz. The field distributions in both parts are in the phase indicated by the amount and magnitude of the H-field vector distribution in the upper cavity. The upper quarter cavity itself is more dominant than the lower cavity. The combination of the weak first mode TE_{101} and the strong second mode TE_{102} results in hybrid-mode resonance at 3.8 GHz, as shown in Figures 5(a) and 6(a). Although the fields distributed in the two cavities are out of phase, their great difference in magnitude can make the triangular slot radiate effectively. Figures 5(b) and 6(b) show that the

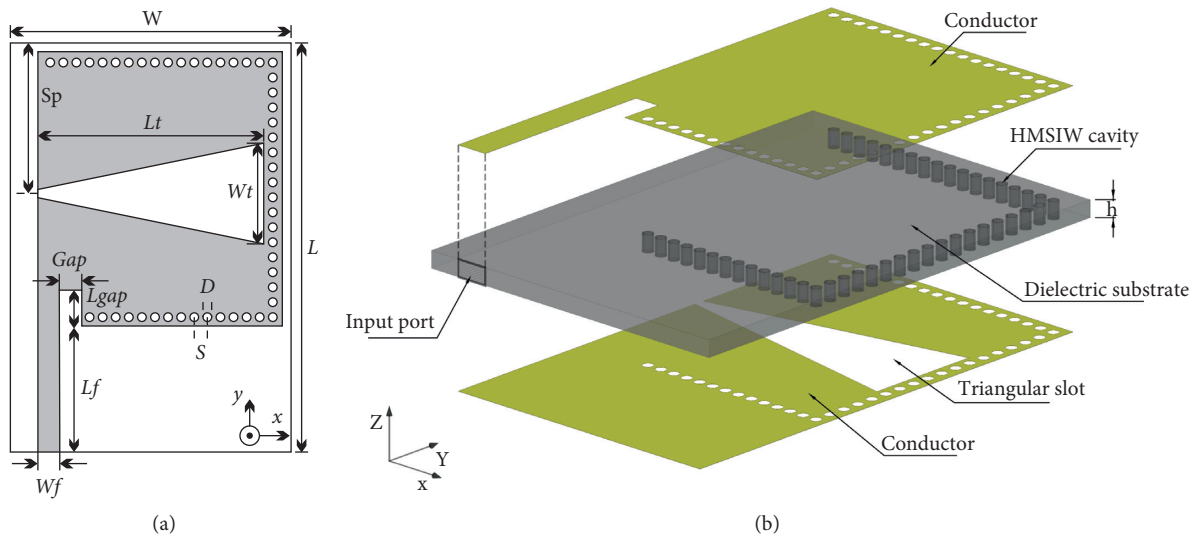

Figure 1: (a) HMSIW-CBS antenna with hybrid resonances using a triangular slot ($W = 31$ mm, $L = 45.5$ mm, $D = 1$ mm, $Sp = 16.75$ mm, $Lt = 25$ mm, $Wt = 11$ mm, $Gap = 2.5$ mm, $Lgap = 4$ mm, $Lf = 14$ mm, and $Wf = 2.425$ mm). (b) Explode view of the proposed HMSIW-CBS antenna.

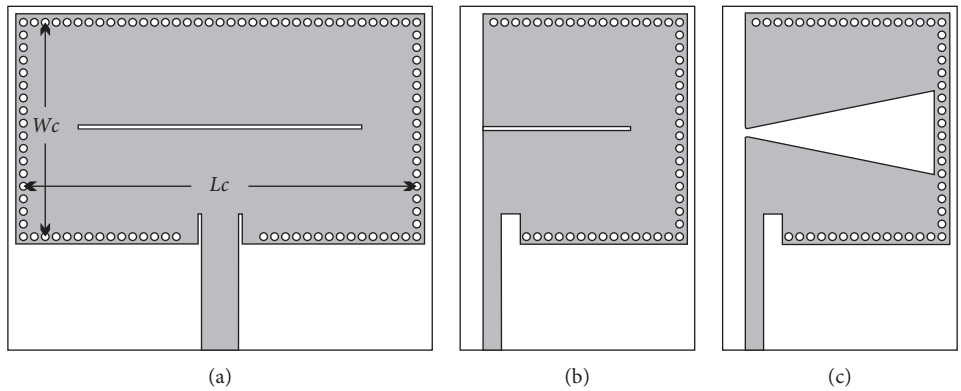

Figure 2: Design evolution of an SIW-CBS antenna for miniaturization and bandwidth enhancement: (a) FMSIW-CBS antenna with a single resonance and (b, c) HMSIW-CBS antenna with hybrid resonances.

hybrid-mode resonances at 3.98 GHz are the combination of a strong first mode TE_{101} and a weak second mode TE_{102}. The magnitudes of the field vector distributions are in phase. As a result, the triangular slot can radiate electromagnetic waves. This investigation follows the methodology given in [7].

3.2. Parametric Analysis. A parametric study of the proposed antenna, as depicted in Figure 1, was conducted to investigate the effects of the position *Sp*, the width *Wt*, and the length *Lt* of the triangular slot on the impedance bandwidth parameter. Figure 7 shows the simulation results for the variations in the reflection coefficient with changes in the position *Sp* of the triangular slot. As mentioned before, the two hybrid modes depend on the quarter cavity parts separated by the triangular slot position *Sp*. Two hybrid modes would be achieved between TE_{101} and TE_{102} if the combination between them is in phase or out of phase; this would depend on the position of the triangular slot. If the triangular slot position *Sp* moves to the bottom of the cavity, the first resonant frequency will shift to the higher frequency and the second resonant frequency will disappear. Critical investigations on the H-field vector will appear on both sides of the quarter cavity. Then, the hybrid modes will disappear and become only a single resonance. This means that the impedance bandwidth will be narrow, and the reflection coefficient will improve. The single resonance shifts into the middle of the impedance bandwidth ranges.

The length *Lt* of the triangular slot was designed as more than a quarter wavelength resonant length of the SIW-CBS conventional antenna. The impedance bandwidth and the improvement in the reflection coefficient also depended on the width *Wt* and the length *Lt* of the triangular slot, as shown in Figure 8. Increasing the width of the triangular slot as shown in Figure 8(a) will cause the first and the second

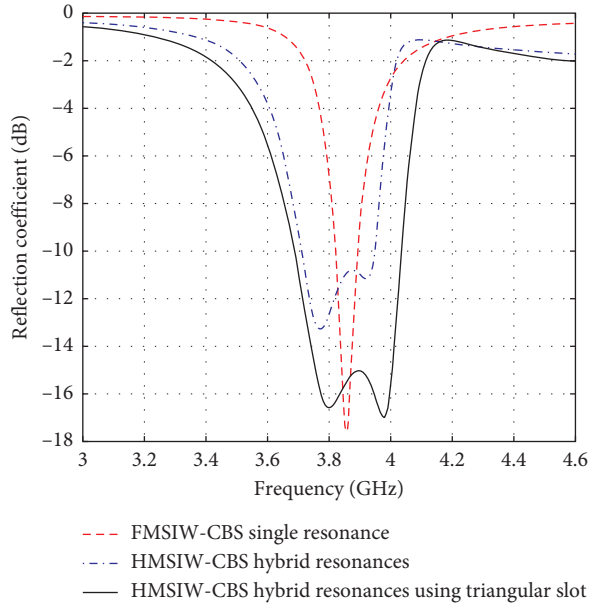

Figure 3: Reflection coefficient for antenna evolution.

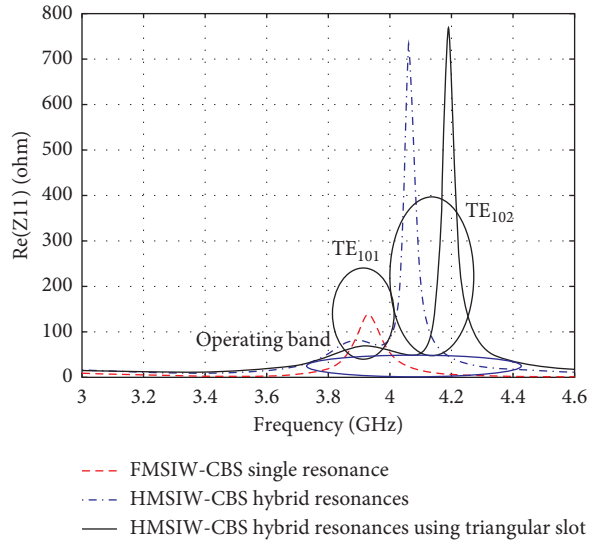

Figure 4: Real impedance (Z_{11}) plot for antenna evolution.

mode resonances to shift to higher frequencies. In addition, the reflection coefficient values will be high and the impedance bandwidth will decrease. The triangular slot width *Wt* of our proposed antenna was chosen to obtain the maximum bandwidth that could be achieved if the slope angle of the triangular slot was 10° [14]. Figure 8(b) reveals that if the triangular slot length increased, the reflection coefficient would be smaller than before. It also causes the impedance bandwidth to become wider than before. The optimum reflection coefficient was chosen to be 25 mm for the triangular slot of length *Lt*.

3.3. Measurement Results. To confirm the simulation studies, the proposed antenna was then fabricated and measured. The fabrication results are exhibited in Figure 9. A triangular slot was etched on the ground layer, and a quarter transmission line was used to connect the current path. All embedded metallic cylinders connected the top layer and the ground layer.

The reflection coefficient of the proposed antenna was validated by the measurement. Figure 10 shows a comparison of the simulation and the measurement of the reflection coefficient. The reflection coefficient for the

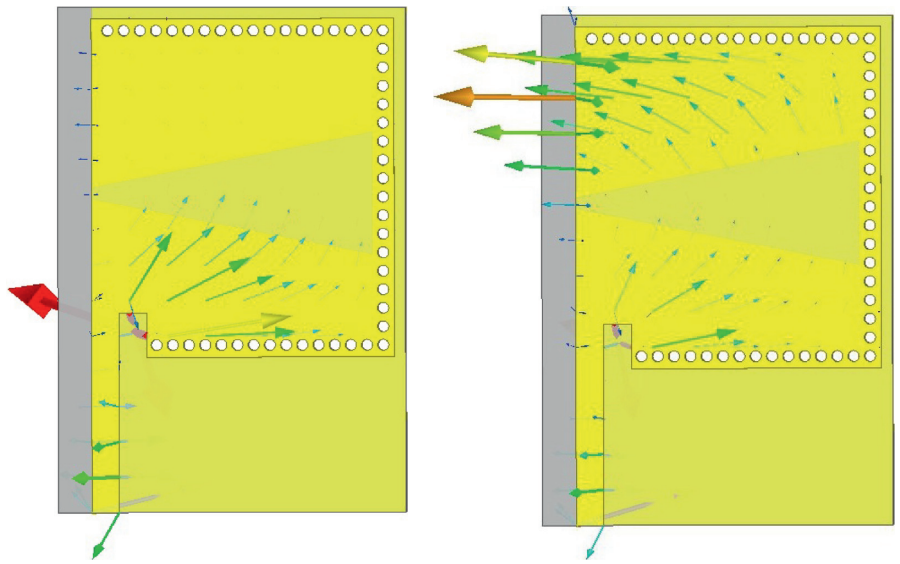

Figure 5: Simulated H-field vector distributions of the hybrid modes in the HMSIW structure at (a) 3.8 GHz and (b) 3.98 GHz.

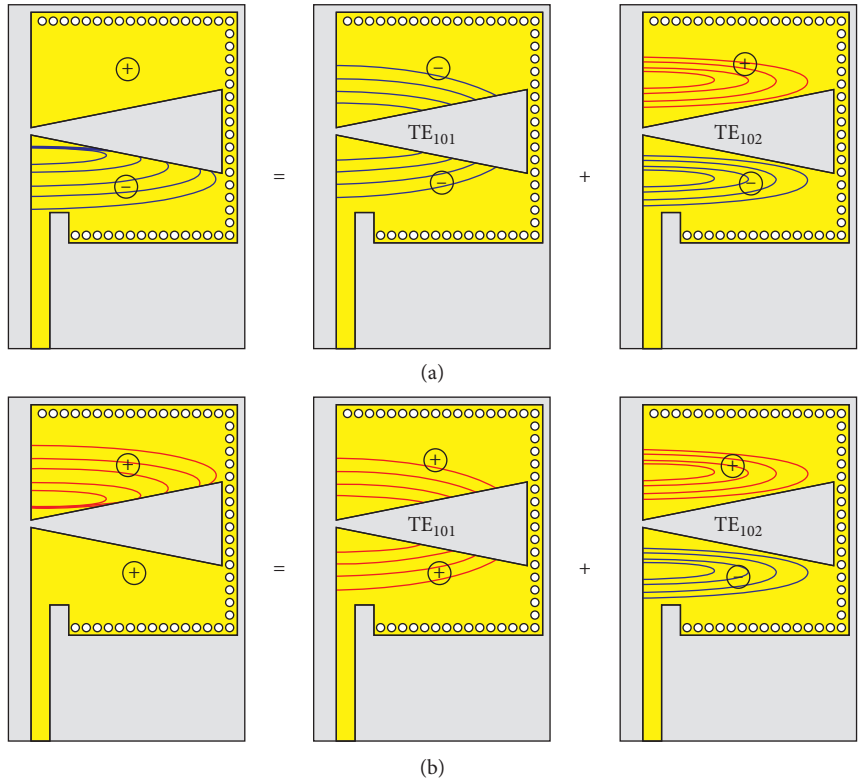

Figure 6: Combination of the simulated dominant E-field between the first mode TE_{101} and the second mode TE_{102} at (a) 3.8 GHz and (b) 3.98 GHz.

simulation shows the proposed antenna functions in the frequency range of 3.69 GHz–4.04 GHz, shown as dashed line. The measurement results for the reflection coefficient are shown by the solid line. The measured fractional bandwidth for VSWR = 2 was 9.87% (3.66–4.04 GHz), and the simulated fractional bandwidth is 9.1%. There was a slight discrepancy between the measurement and simulation results, which was caused by the parasitic effect of the antenna that is influenced by the soldering process in the connector, but overall it can be tolerated.

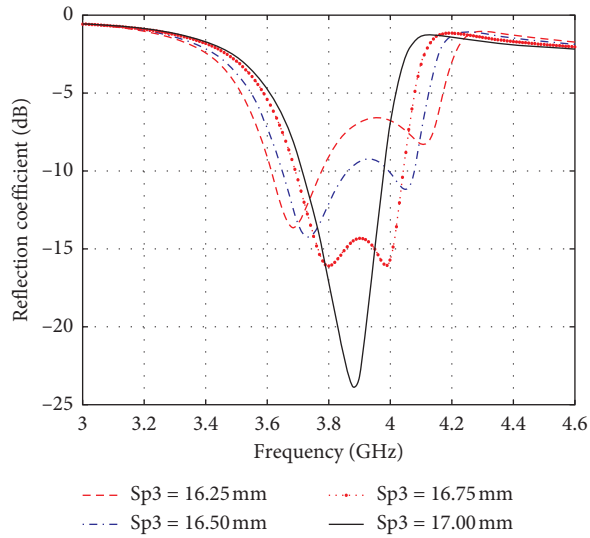

Figure 7: Variations in the reflection coefficient with changes in the slot position (*Sp*).

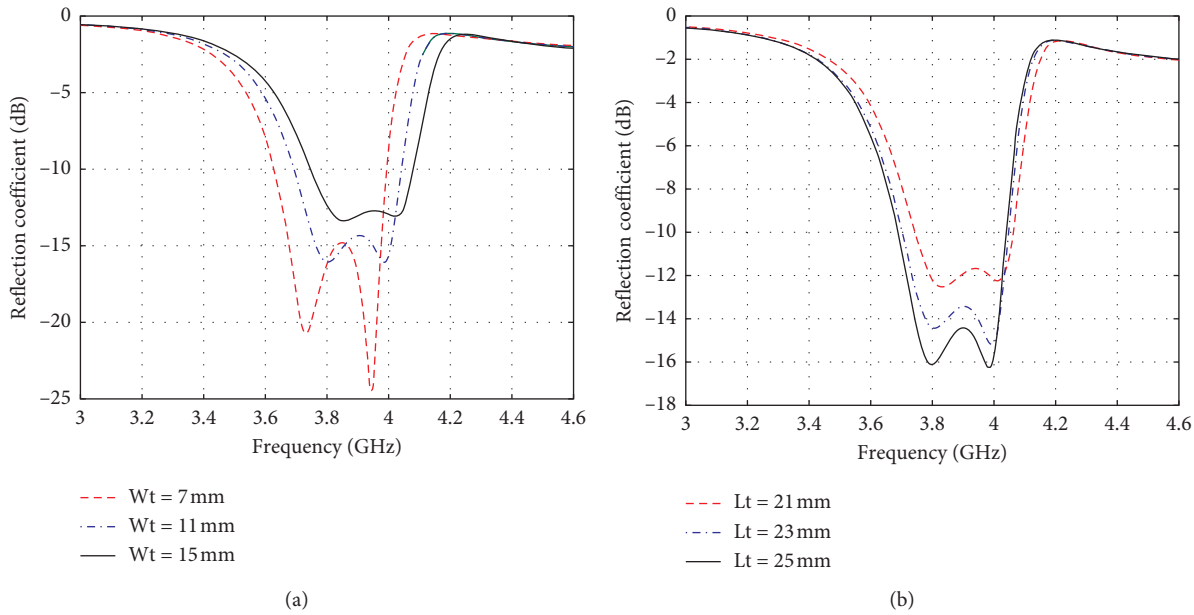

Figure 8: Variations in the reflection coefficient with changes in the (a) triangular slot width (*Wt*) and (b) triangular slot length (*Lt*).

The gain simulation and measurement are shown in Figure 10. The gain measurements for the H-plane were 3.89 dBi and 2.89 dBi at 3.72 GHz and 3.98 GHz, respectively. The gain measurement for the E-plane was 4.2 dBi at both frequencies. The differentiation between simulation and measurement gain occurs because of the measurement condition such as antenna tilt. The simulation and measurement gain that are achieved using the HMSIW structure are not higher than the FMSIW-CBS single resonance because of the HMSIW topology itself.

Figure 11 shows the simulation and measurement radiation pattern performance for the antenna design. The measured frequency used 3.72 GHz and 3.98 GHz, which are the antenna-working frequencies. The measured copolarization and cross-polarization far-field radiation pattern used a horn antenna as the reference antenna. The measurements of the normalized copolarization antenna agreed well for the H-plane (phi = 0°) and E-plane (phi = 90°). The measured copolarization has a unidirectional antenna. This occurs because the electric field of the antenna design has radiation on the patch and the ground plane, even when the difference between them was approximately 10 dB. The E-plane was approximately 90° for the half-power beamwidth antenna, whereas the H-plane was approximately 120° for the half-power beamwidth. The cross-polarization level measurements were −3 dB in the E-plane and −8 dB in the H-plane.

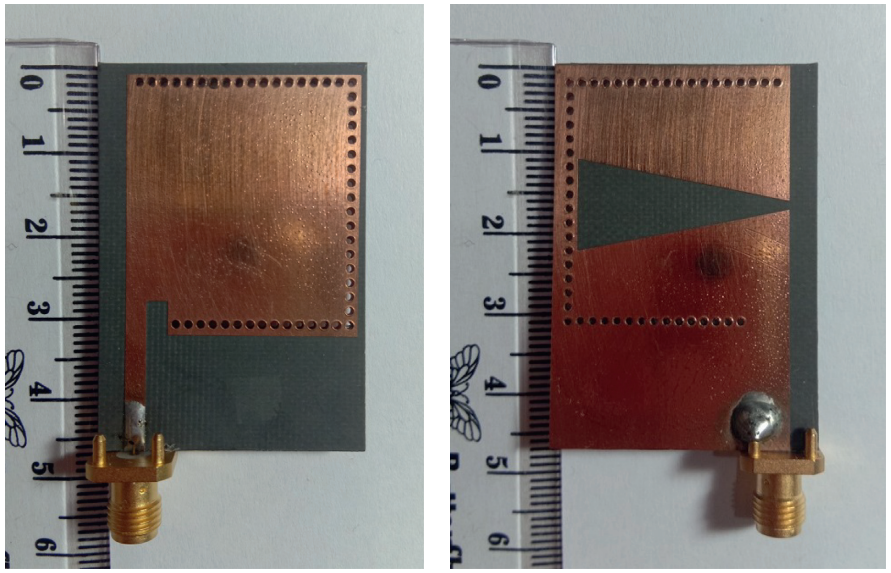

(a) (b)

Figure 9: Prototype of the proposed SIW-CBS antenna using a triangular slot: (a) top layer and (b) ground layer.

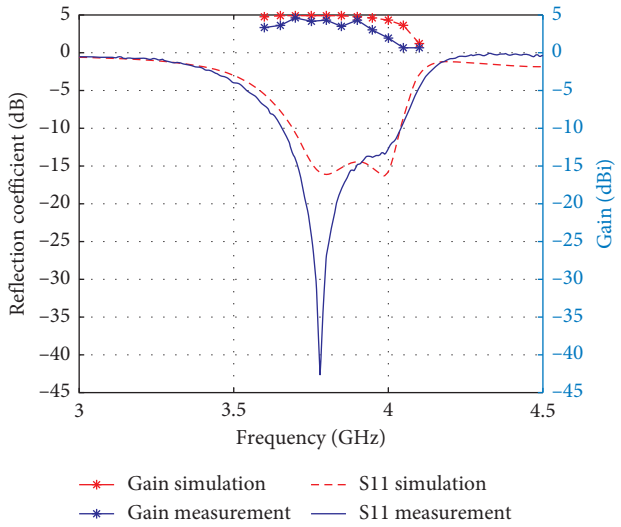

Figure 10: Reflection coefficient for the simulation (dashed line) and the measurement result (solid line).

High cross-polarization levels occurred because of linear polarization impurities.

Finally, Table 1 shows a comparison with previous results related to the miniaturization and bandwidth enhancement of the CBS antenna. The HMSIW structure was an effective method for miniaturization. Approximately 50% miniaturization of the antenna design was achieved using the HMSIW structure without decreasing the fractional bandwidth, and the triangular slot on the ground layer enhances the fractional bandwidth of the CBS antenna. Table 1 reveals that this study has achieved bandwidth enhancement up to 9.87% from the conventional SIW-CBSA with miniaturization dimension compared with other studies. Reference [8] reported bandwidth enhancement similar to that in this study, but the dimension is still large because of the use of FMSIW-CBSA.

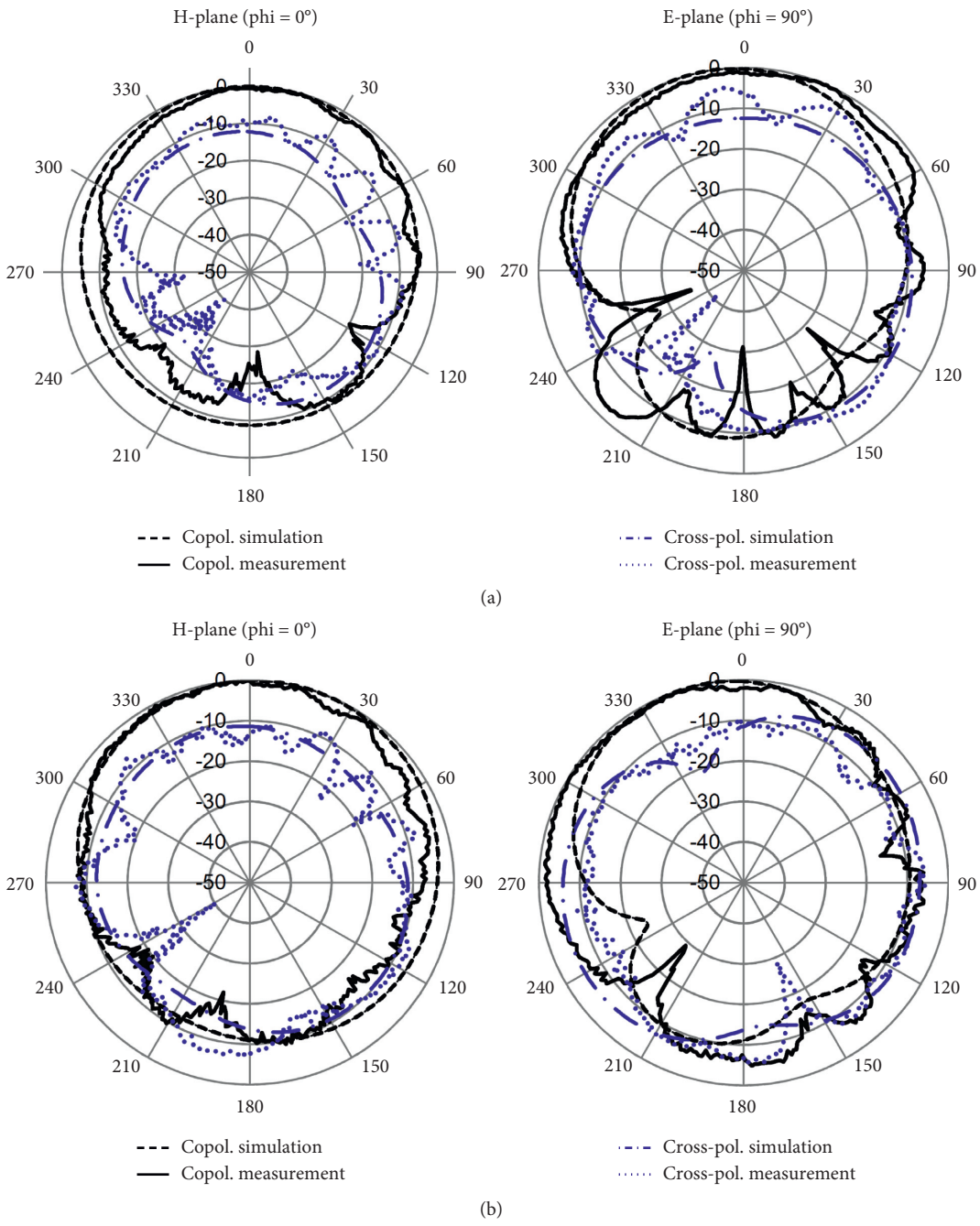

Figure 11: Simulation and measurement results of radiation patterns for (a) 3.72 GHz and (b) 3.98 GHz.

Table 1: Comparison with previous studies with respect to the bandwidth enhancement of the CBS antenna.

Reference	Fc (GHz)	FBW (%)	Gain (dBi)	Antenna dimension
[1]	8.58	4.9	6.7	$3.73\times10^{-1}\ \lambda_0^3$
[2]	8.75	6	4.87	$3\times10^{-3}\ \lambda_0^3$
[3]	2.45	1.22	3.64	$5.7\times10^{-10}\lambda_0^3$
[4]	5.82	3.78	5.25	$3.86\times10^{-1}\ \lambda_0^3$
[6]	2.45	2.16	NA	$2.62\times10^{-4}\ \lambda_0^3$
[7]	2.45	3.35	5	$3.06\times10^{-3}\ \lambda_0^3$
[8]	10	6.32	6	$4.01\times10^{-3}\ \lambda_0^3$
[9]	10	9.43	3.53–5.4	$8.29\times10^{-3}\ \lambda_0^3$
This work	3.84	9.87	4.2	$2.55\times10^{-1}\ \lambda_0^3$

4. Conclusions

In this study, the bandwidth enhancement of a HMSIW-CBS using a triangular slot structure antenna has been studied for simulation and measurement. It shows that bandwidth enhancement was influenced by the position, length, and width of the triangular slot. The appropriate combination of position, length, and width of the slot can generate the hybrid mode between the TE_{101} and TE_{102} modes, which depends on the phases of TE_{101} and TE_{102} modes. With the proposed method, an increase in fractional bandwidth of up to 9.87% from the conventional SIW-CBS was achieved. It is also shown that the fractional bandwidth increases up to 5.45 times than the conventional SIW-CBS.

Data Availability

The data used in this study are available upon request to the corresponding author.

Conflicts of Interest

The authors declare no conflicts of interest.

Acknowledgments

The authors would like to thank Universitas Indonesia for supporting the research funding Hibah Tugas Akhir Mahasiswa Doktor (TADOK 2019) under contract NBK-0161/UN2.R3.1/HKP.05.00/2019.

References

[1] S. A. Razavi and M. H. Neshati, "Development of a linearly polarized cavity-backed antenna using HMSIW technique," *IEEE Antennas and Wireless Propagation Letters*, vol. 11, pp. 1307–1310, 2012.

[2] S. A. Razavi and M. H. Neshati, "Development of a low-profile circularly polarized cavity-backed antenna using HMSIW technique," *IEEE Transactions on Antennas and Propagation*, vol. 61, no. 3, pp. 1041–1047, 2013.

[3] D. W. Astuti and E. T. Rahardjo, "Size reduction of cavity backed slot antenna using half mode substrate integrated waveguide structure," in *Proceedings of the 4th International Conference Nano Electron. Research Education Towards Advances in Imaging Science Creation ICNERE*, pp. 1–4, Shizuoka, Japan, November 2018.

[4] D. Chaturvedi and S. Raghavan, "A half-mode SIW cavity-backed semi-hexagonal slot antenna for WBAN application," *IETE Journal of Research*, vol. 65, no. 11, pp. 1–7, 2018.

[5] S. Yun, D. Y. Kim, and S. Nam, "Bandwidth and efficiency enhancement of cavity-backed slot antenna using a substrate removal," *IEEE Antennas and Wireless Propagation Letters*, vol. 11, pp. 1458–1461, 2012.

[6] S. Yun, D. Y. Kim, and S. Nam, "Bandwidth enhancement of cavity-backed slot antenna using a via-hole above the slot," *IEEE Antennas and Wireless Propagation Letters*, vol. 11, pp. 1092–1095, 2012.

[7] G. Q. Luo, Z. F. Hu, W. J. Li, X. H. Zhang, L. L. Sun, and J. F. Zheng, "Bandwidth-enhanced low-profile cavity-backed slot antenna by using hybrid SIW cavity modes," *IEEE Transactions on Antennas and Propagation*, vol. 60, no. 4, pp. 1698–1704, 2012.

[8] S. Mukherjee, A. Biswas, and K. V. Srivastava, "Broadband substrate integrated waveguide cavity-backed bow-tie slot antenna," *IEEE Antennas and Wireless Propagation Letters*, vol. 13, pp. 1152–1155, 2014.

[9] D. M. Pozar, *Microwave Engineering*, Wiley, New York, NY, USA, 4th edition, 2012.

[10] M. Bozzi, A. Georgiadis, and K. Wu, "Review of substrate-integrated waveguide circuits and antennas," *IET Microwaves, Antennas & Propagation*, vol. 5, no. 8, pp. 909–920, 2011.

[11] X.-P. Chen and K. Wu, "Substrate integrated waveguide filter: basic design rules and fundamental structure features," *IEEE Microwave Magazine*, vol. 15, no. 5, pp. 108–116, 2014.

[12] X.-P. Chen and K. Wu, "Substrate integrated waveguide filters: design techniques and structure innovations," *IEEE Microwave Magazine*, vol. 15, no. 6, pp. 121–133, 2014.

[13] F. Xu and K. Wu, "Guided-wave and leakage characteristics of substrate integrated waveguide," *IEEE Transactions on Microwave Theory and Techniques*, vol. 53, no. 5, pp. 66–73, 2005.

[14] J.-F. Huang and C.-W. Kuo, "CPW-fed bow-tie slot antenna," *Microwave and Optical Technology Letters*, vol. 19, no. 5, pp. 358–360, 1998.